



Solar FTIR measurements of NO_x vertical distributions – Part 2: Experiment-based scaling factors describing the daytime variation in stratospheric NO_x

Pinchas Nürnberg¹, Sarah A. Strode^{2,3}, and Ralf Sussmann¹

¹IMK-IFU, Karlsruhe Institute of Technology, Garmisch-Partenkirchen, Germany

²Goddard Earth Sciences Technology and Research (GESTAR II), Morgan State University,
Baltimore, MD 21251, USA

³NASA Goddard Space Flight Center, Greenbelt, MD 20771, USA

Correspondence: Pinchas Nürnberg (pinchasnuernberg@web.de) and Ralf Sussmann
(ralf.sussmann@kit.edu)

Received: 30 June 2023 – Discussion started: 1 November 2023

Revised: 5 April 2024 – Accepted: 11 July 2024 – Published: 10 September 2024

Abstract. Long-term experimental stratospheric NO_2 and NO partial columns measured by means of solar Fourier-transform infrared (FTIR) spectrometry at Zugspitze (47.42° N, 10.98° E; 2964 m a.s.l.), Germany, were used to create a set of experiment-based monthly scaling factors (SF_{exp}). The underlying data set is published in a companion paper (Nürnberg et al., 2024) and comprises over 25 years of measurements depicting the daytime variability of stratospheric NO_2 and NO partial columns with respect to local solar time (LST). In accordance with simulation-based scaling factors recently published by Strode et al. (2022), we created SF_{exp} normalized to $\text{SZA} = 72^\circ$ for NO_2 and NO for every month of the year as a function of solar zenith angle (SZA). Apart from a boundary value problem at minimum SZA values originating from averaging over different times of the month, the obtained scaling factors $\text{SF}_{\text{exp}}(\text{NO}_2)$ and $\text{SF}_{\text{exp}}(\text{NO})$ as a function of SZA represent the daytime behavior already shown in model simulations and experiments in the literature very well. This shows a well-pronounced increase in the NO_2 and NO stratospheric partial column with the time of the day and a flattening of this increase after noon. In addition to the discussion of SF_{exp} , we validate the simulation-based scaling factors $\text{SF}_{\text{sim}}(\text{NO}_2)$ (Strode et al., 2022) and present simulation-based scaling factors for NO $\text{SF}_{\text{sim}}(\text{NO})$. The simulation-based scaling factors show excellent agreement with the experiment-based ones; i.e., for NO_2 and NO the mean value of the modulus between the experiment and simulation over all SZAs and months is only 0.02 %. We show that recently used model simulations can describe the real behavior of nitrogen oxide (NO_x) variability in the stratosphere very well. Furthermore, we conclude that ground-based FTIR measurements can be used for validation of the output of photochemistry models and for creating experiment-based data sets describing the daytime stratospheric NO_x variability as a function of SZA. This is a contribution to improved satellite validation and a better understanding of stratospheric photochemistry.

1 Introduction

The important role of NO₂ and NO in stratospheric photochemistry has been known for half a century (Crutzen, 1979). Both nitrogen oxides (NO_x) are a product of the photolysis of N₂O and are an important part of the ozone (O₃)-destroying nitrogen catalytic cycle which controls the O₃ abundance in the stratosphere (Johnston, 1992). Additionally, industry and transportation are major sources of tropospheric NO_x in the troposphere (Grewe et al., 2001). In urban areas in particular, NO_x can serve as a precursor for, e.g., O₃ or nitric acid (HNO₃) and can therefore promote smog events and directly affect human health (World Health Organization, Regional Office for Europe, 2003). Furthermore, NO₂ has the potential to cause significant radiative forcing during pollution events with highly elevated NO₂ concentrations in the troposphere (Solomon et al., 1999).

The monitoring and quantification of NO_x total columns have been conducted since 1967 via different satellite missions (Godin-Beekmann, 2010; Rusch, 1973). Therefore, for the observation of tropospheric pollution events (e.g., smog), knowledge of the stratospheric contribution to the total column is crucial. One way to face this problem is the reference sector method, taking unpolluted total columns at a similar latitude (e.g., above the ocean) as a reference and subtracting them from the total column (Richter and Burrows, 2002). The two main assumptions justifying this approach are the longitudinal homogeneity of the stratospheric column and negligible tropospheric columns over the ocean. However, due to the strong diurnal cycle of NO₂ and NO, no time mismatch should occur between both columns.

One method for dealing with the problem of time and site mismatches when comparing different NO_x columns is the use of ground-based Fourier-transform infrared (FTIR) measurements. This method can provide data from any time of the day during sunlight hours, giving the opportunity to describe daytime NO_x variabilities with a high precision, as done for NO₂ by Sussmann et al. (2005). For the first time, they found a reliable daytime NO₂ increasing rate of $(1.02 \pm 0.12) \times 10^{14} \text{ cm}^{-2} \text{ h}^{-1}$ derived from FTIR measurements at midlatitudes. Additionally, the retrieved FTIR data can have a certain altitude resolution, which allows for conclusions about NO_x partial column variabilities to be made, e.g., of the stratospheric columns (Zhou et al., 2021; Yin et al., 2019). In our companion paper, Part 1 (Nürnberg et al., 2024), we used these advantages of ground-based FTIR measurements to retrieve stratospheric partial columns from long-term NO₂ and NO measurements above Zugspitze (47.42° N, 10.98° E; 2964 m a.s.l.), Germany, yielding information on NO_x daytime variability for every month of the year. This specific data set has the potential to improve satellite validation and can serve as a basis for the description of stratospheric NO_x variabilities with high time resolution. However, the data from ground-based measurements can only be retrieved for the limited number and locations of existing sites.

A method without this site restriction describing stratospheric NO_x concentrations with global coverage is the use of model data from three-dimensional global transport and photochemistry models. The latter is able to describe trace gas concentrations with respect to altitude, latitude and longitude with a very good time resolution. In comparison to one-dimensional models describing only the vertical distribution of atmospheric trace gases (e.g., O₃, NO₂, NO) (Allen et al., 1984; Prather and Jaffe, 1990), three-dimensional models simulate transport fluxes in all three dimensions and are able to include nearly all feedback mechanisms of the real world (McLinden et al., 2000; Chang and Duewer, 1979). Both types of models can account for daytime variabilities and have been used in the last few decades for inter-satellite comparisons (Brohede et al., 2007; Dubé et al., 2020) as well as for satellite data validation (Bracher et al., 2005) and correction (Dubé et al., 2021; Wang et al., 2020). However, these studies differ from case to case and do not provide general global information about NO_x variability. This global information should be site independent and can be applied to any satellite validation or correction all over the planet.

Here, a recent study of Strode et al. (2022) closed this gap by developing a set of simulation-based scaling factors (SF_{sim}), which describe the daytime variability of NO₂. A given SF_{sim} is a measure of the change in trace gas concentrations during the day normalized to a specific time (here sunrise or sunset). SF_{sim} factors are extracted from a three-dimensional model, which considers long-range transport, stratospheric and tropospheric chemistry, aerosol, radiation, and transport. The generated monthly output is available for latitudes between −90 and 90° (1° steps) and altitudes between 6 and 78 km (0.5 km steps) for every time of the day given in solar zenith angle (SZA) values (Strode et al., 2022). This extensive research provides the opportunity for the comparison, validation and correction of remote and ground-based data products by overcoming time or site mismatches.

However, an observational counterpart, i.e., an analogous data set of experiment-based scaling factors describing the daytime increase in stratospheric NO_x, still does not exist due to the lack of reliable long-term data comprising the full daytime NO₂ and NO variability. To close this gap, in this paper we create a set of experiment-based scaling factors (SF_{exp}), analogous to the simulation-based scaling factors published by Strode et al. (2022). On the one hand, this data set should serve as a general set of data describing the NO_x daytime variability with respect to SZA for the given latitude (47° N) of our observation site. On the other hand, we would like to use the data set to validate the recently published model data for SF_{sim}(NO₂) (Strode et al., 2022) and unpublished model data for SF_{sim}(NO) (Sarah Strode, personal communication, 2023). For this SF_{exp} data set, we use the observational results described in Part 1 (Nürnberg et al., 2024), where a reliable long-term data set of NO₂ and NO partial columns above 16 km altitude above Zugspitze was created. As described above, these long-term data are

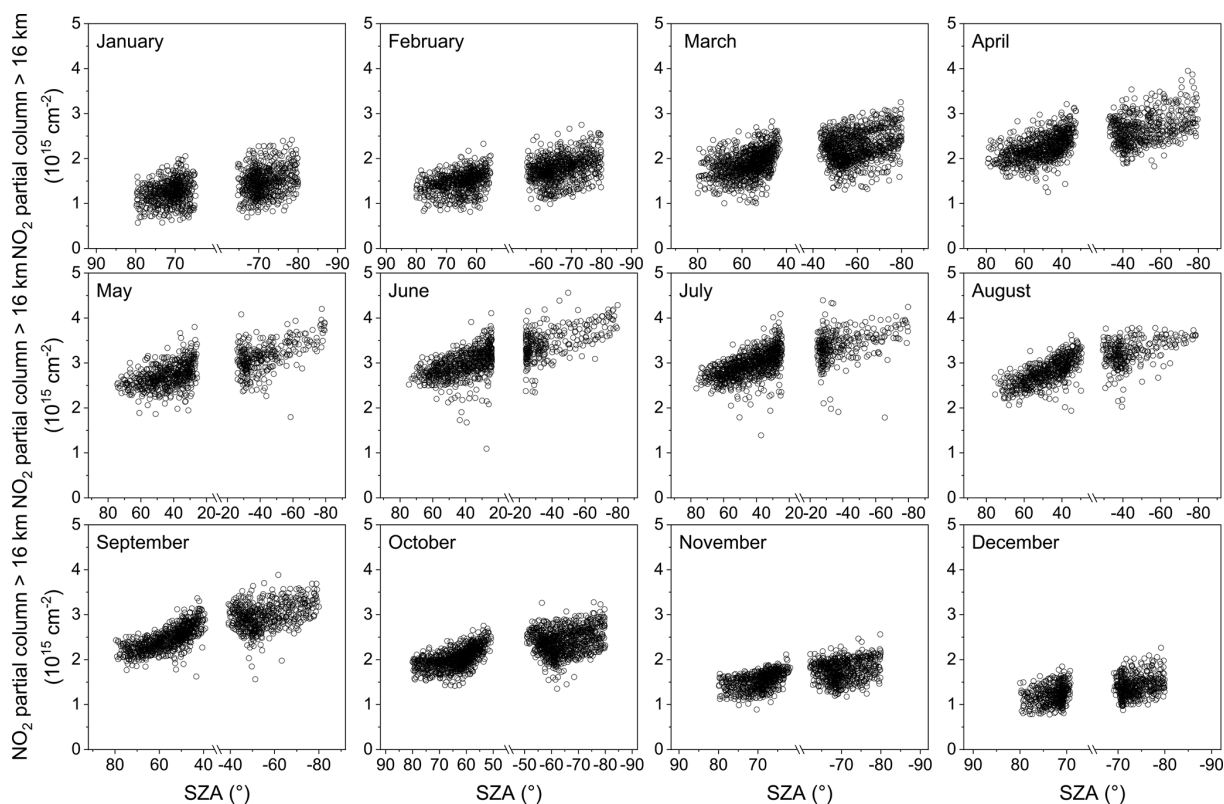


Figure 1. Retrieved NO₂ partial column above 16 km altitude measured at Zugspitze (black symbols) for every month with respect to SZA.

retrieved from ground-based FTIR measurements and describe the daytime variability of stratospheric NO_x within time steps of minutes for every month of the year. The cutoff point at 16 km was chosen to avoid influences of variabilities near the tropopause and in the boundary layer upon the stratospheric partial column. Details are discussed in Part 1. It is outside the scope of this work to describe the strong and fast photochemistry at sunrise and sunset with SF_{exp}.

In Sect. 2, this paper (Part 2 of our companion paper) briefly describes the experimental setup and the resulting FTIR data taken from Part 1 (Nürnberg et al., 2024). In Sect. 3, the dependence on SZA for NO₂ and NO is shown, and the resulting daytime variations presented in detail in Part 1 are discussed briefly before the NO_x partial columns (> 16 km) are converted into experiment-based scaling factors (SF_{exp}(NO₂) and SF_{exp}(NO)) in Sect. 4. Finally, the resulting SF_{exp} factors are compared qualitatively and quantitatively to SF_{sim} retrieved from model simulations.

2 FTIR data

All data of this study are retrieved from long-term ground-based FTIR solar absorption measurements at Zugspitze, Germany (47.42° N, 10.98° E; 2964 m a.s.l.). The high-altitude observatory at Zugspitze is located in the German Alps and can be regarded as a clean site without strong in-

fluences from pollution events in the boundary layer. The Bruker IFS 125HR spectrometer used in this study has been operating continuously since 1995 at Zugspitze. The experimental setup and retrieval strategy are described in the companion paper (Nürnberg et al., 2024). As described in Part 1, we used daily pressure and temperature profiles from the National Centers for Environmental Prediction (NCEP) interpolated to the measurement time. The temperature dependency of the data cannot be discussed in detail here, but it is very likely that the stratospheric temperature affects the NO_x concentration and therefore also the observed diurnal cycle. The pollution-filtered NO and NO₂ stratospheric partial columns (above 16 km altitude) derived in our Part 1 study serve as a basis for the experiment-based scaling factors created now in this Part 2 work. The data set comprises 6213 NO and 16 023 NO₂ partial columns measured at Zugspitze between 1995 and 2022.

3 Experimental data

NO_x stratospheric partial column dependence on SZA

Figure 1 shows the NO₂ stratospheric partial columns (black symbols) taken from Nürnberg et al. (2024) for every month as a function of SZA. Note this is the same data as shown in our Part 1 (Fig. 3 therein), which had been plotted as a

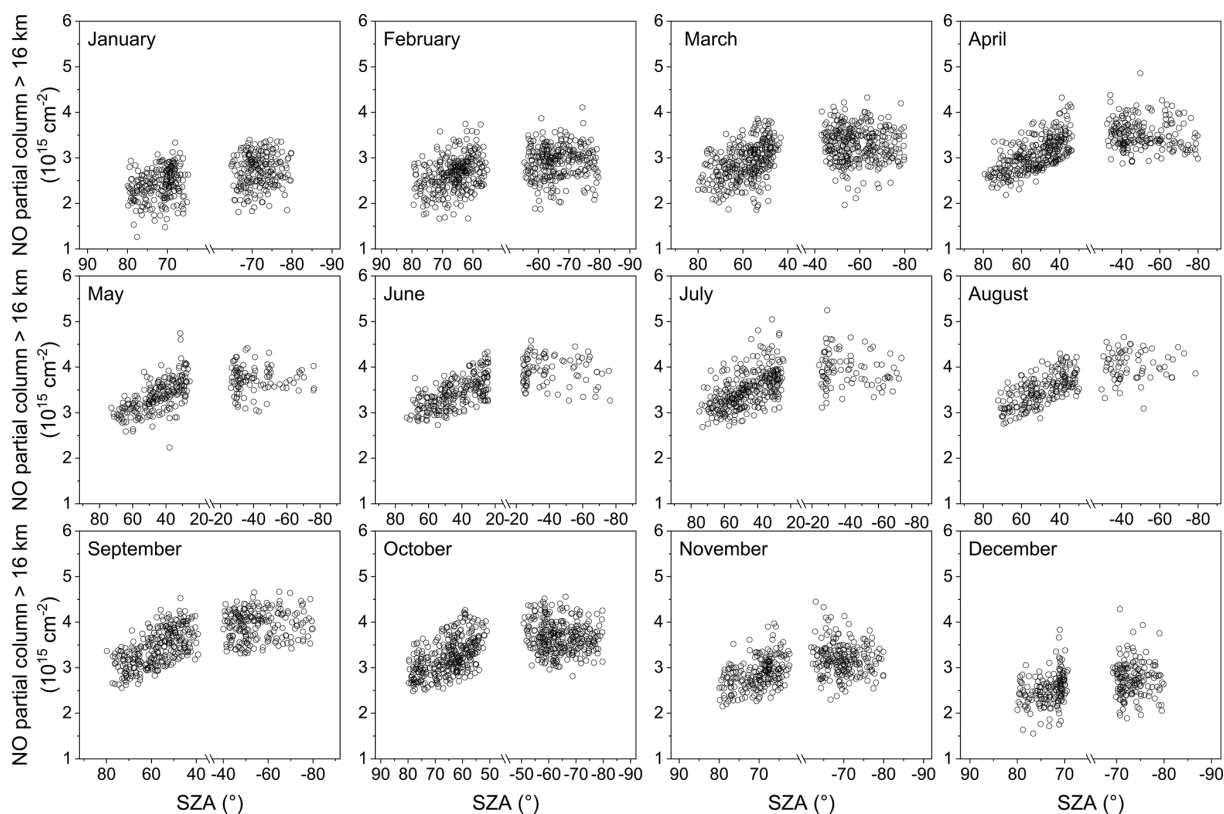


Figure 2. Retrieved NO partial column above 16 km altitude measured at Zugspitze (black symbols) for every month with respect to SZA.

function of local solar time. The x axis is interrupted for SZA values without observations in the respective month. Here, we define SZA to be positive in the morning from sunrise ($\text{SZA} = 90^\circ$) to local solar noon (respective minimum value dependent on the season) and to be negative in the afternoon between local solar noon and sunset ($\text{SZA} = -90^\circ$).

As already described and discussed in Part 1, the daytime increase in the NO₂ stratospheric partial column follows for every month a linear behavior from sunrise to sunset. Briefly, this behavior reflects the photolysis of the reservoir species HNO₃ and N₂O₅, resulting in a consecutive increase in NO₂ during daytime (Crutzen, 1970).

Similarly, Fig. 2 shows the NO stratospheric partial columns (black symbols) taken from the same work for every month with respect to SZA (Nürnberg et al., 2024). Note this is the same data as shown in our Part 1 (Fig. 5 therein) as a function of local solar time. Briefly, the data show the typical daytime increase in stratospheric NO described in the literature via model calculations (Dubé et al., 2020; McLinden et al., 2000) or shown experimentally (Zhou et al., 2021; Rinsland et al., 1984) for every month. Here, the photolysis of the reservoir species N₂O leads to a well-pronounced increase in the stratospheric NO concentration in the morning (Crutzen, 1970). After local solar noon, the shift in the NO₂–NO equilibrium, the increasing amount of O₃ and the solar elevation dependency of the involved photochemical reaction lead to

a strong flattening of the daytime NO curve as a function of SZA in comparison to NO₂. This afternoon effect is more pronounced in the summertime (middle row) than in the rest of the year (Nürnberg et al., 2024).

4 Calculation of experiment-based scaling factors

A set of experiment-based scaling factors (SF_{exp}) analogous to the model-based scaling factors (SF_{sim}) published by Strode et al. (2022) was created as follows: the mean values for 2° bins of SZA of the stratospheric partial column (> 16 km) were calculated. In a next step, these mean values were normalized to $\text{SZA} = 72^\circ$ (which is the only value that is present in all monthly data sets), resulting in monthly SF_{exp} sets for NO₂ and NO shown in Figs. 3 and 4, respectively. These data reflect the daytime variation in stratospheric NO₂ and NO above Zugspitze, Germany. Values resulting from only one measurement point are shown in red without error bars.

$\text{SF}_{\text{exp}}(\text{NO}_2)$ (Fig. 3, black and orange symbols) increases linearly throughout the day in each month, reflecting the increase in the stratospheric NO₂ concentration. There are two observations which can be pointed out here. First, the error bars in Fig. 3 (i.e., ± 2 standard errors of the mean, $\pm 2 \text{SEM} = \pm 2\sigma/\sqrt{(n)}$) are independent of the season and are very small, reflecting a low scattering within the 2° SZA bins and

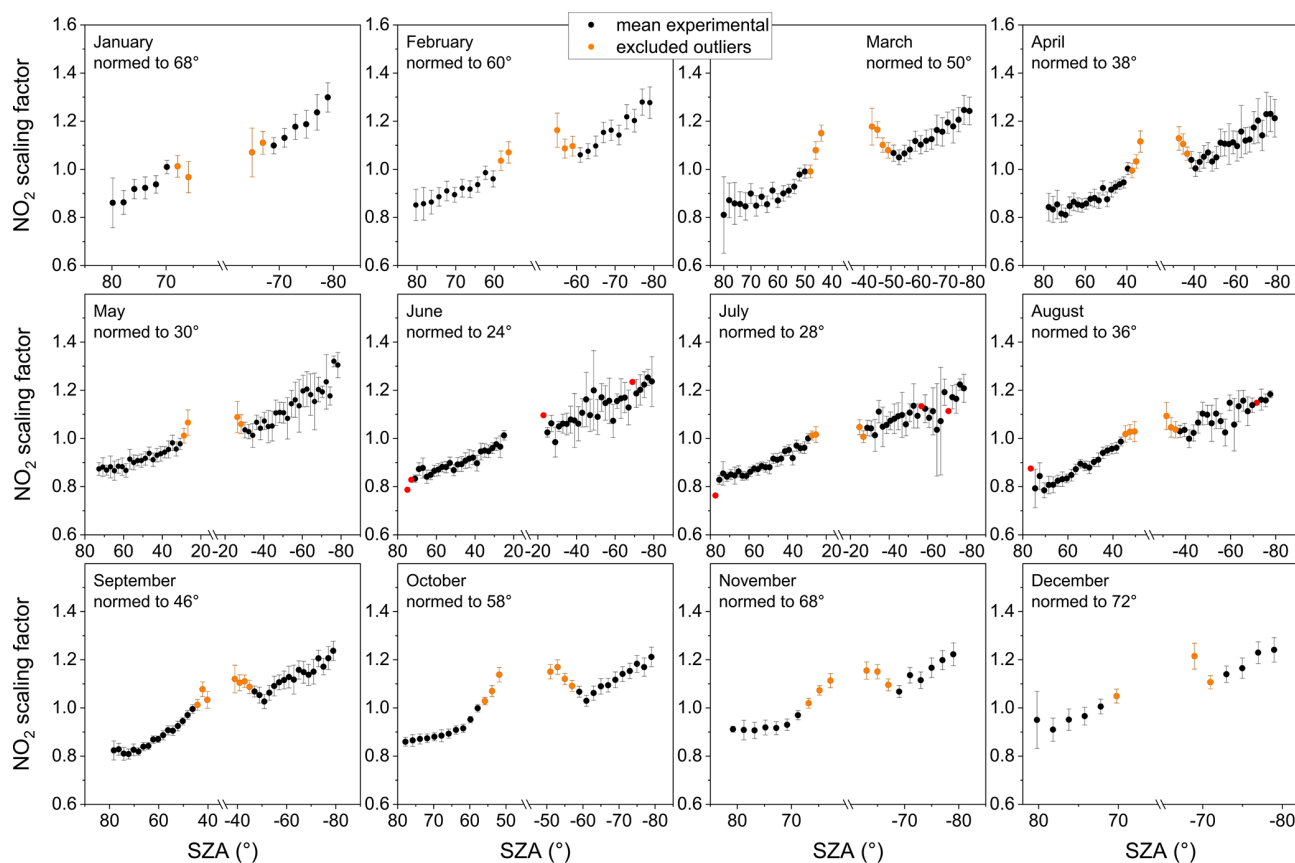


Figure 3. Calculated normalized NO₂ scaling factors $SF_{\text{exp}}(\text{NO}_2)$ above 16 km altitude measured at Zugspitze (black; orange symbols are excluded outliers) for every month with respect to the SZA. The values represent the mean value within 2° SZA bins. The error bars represent 2 times the standard error of the mean ($\pm 2\sigma/\sqrt{n}$) value. Values resulting from only one measurement point are shown in red without error bars.

enough averaging data points n . Second, in spring and autumn, at local solar noon (minimum SZA), a significant increase in $SF_{\text{exp}}(\text{NO}_2)$ is visible. This effect can be understood as a boundary value problem being due to the relatively fast change in SZA and the NO₂ stratospheric partial column (seasonal variation) during the spring and autumn months, respectively. Here, the combination of both the SZA and the stratospheric partial column changes within 1 month results in an increased averaged NO₂ stratospheric partial column near the minimum SZA. The reason is that for SZA values below the minimum SZA at day 15 of each month, only partial columns from one half of the month can contribute to the average. Unfortunately, the stratospheric partial columns of this half deviate significantly from the monthly mean. Figure S1 in the Supplement illustrates this phenomenon using the NO₂ partial column above 16 km altitude. Here, the first half (red symbols) and the second half (blue symbols) of April are split up into two data sets underlining the described boundary value problem. At low SZA values, only blue data points sum up to the averaged values, considering only the second half of the month. Consequently, the partial column

and, of course, the scaling factor increase artificially (pointed out by the blue arrow in the figure). This effect leads us to the exclusion of these data points (Fig. 3, orange symbols) below the minimum SZA reached at day 15 of the respective month. Another opportunity to face this problem would be the choice of a smaller time binning (e.g., 2 weeks, 10 d). However, this would (i) worsen the comparability to the simulation-based scaling factors and (ii) reduce the usable data base per time bin. The entire data set of $SF_{\text{exp}}(\text{NO}_2)$ can be found in the Supplement Tables S1–S4.

For $SF_{\text{exp}}(\text{NO})$ (Fig. 4, black and orange symbols), the difference in daytime increase in comparison to NO₂ is very well pronounced. Before local solar noon, SF_{exp} increases for every month linearly. After local solar noon, the described flattening of the increase is visible. Here, the NO stratospheric partial column stays almost constant within the scattering until sunset, independent of the season. The ± 2 SEM error bars of $SF_{\text{exp}}(\text{NO})$ shown in Fig. 4 are also very small, but more values are excluded (red symbols) due to the availability of only one measurement point within the corresponding 2° SZA bin. This reflects the lower data base of the NO

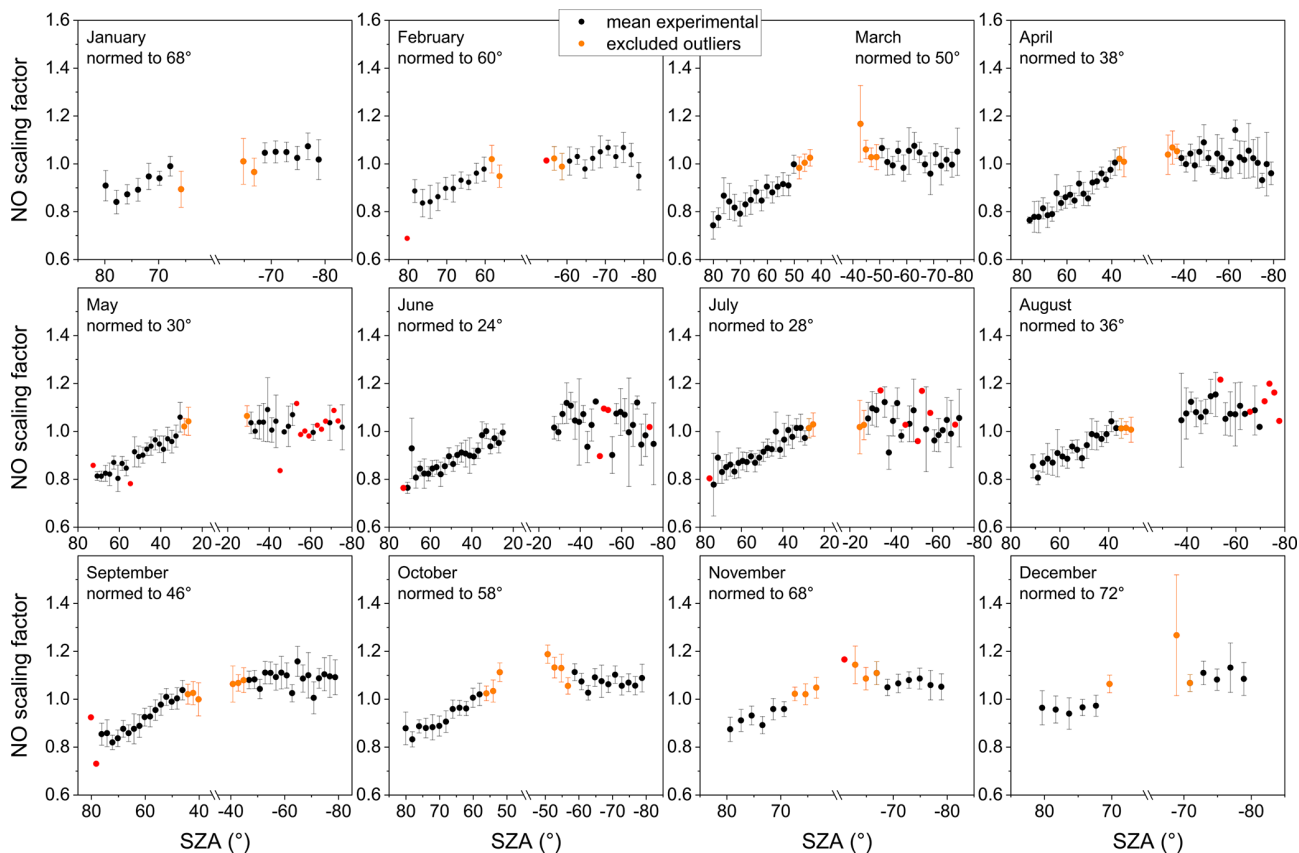


Figure 4. Calculated normalized NO scaling factors $SF_{\text{exp}}(\text{NO})$ above 16 km altitude measured at Zugspitze (black; orange symbols are excluded outliers) for every month with respect to SAZ. The values represent the mean value within 2° SAZ bins. The error bars represent 2 times the standard error of the mean ($\pm 2\sigma/\sqrt{n}$) value. Values resulting from only one measurement point are shown in red without error bars.

retrieval, originating from the use of another spectral micro-window for analysis. However, the small error bars underline that for most of the mean values, the data base is reliable. A similar but even less pronounced effect can be seen near local solar noon for $SF_{\text{exp}}(\text{NO})$, as described for NO_2 . Here, the deviation from the visible trend in spring or autumn months is very small. However, for consistent data handling we also exclude the respective values (orange symbols) for $SF_{\text{exp}}(\text{NO})$ below the minimum SAZ at each month on the 15th. The entire data set of $SF_{\text{exp}}(\text{NO})$ can be found in Tables S5–S8.

5 Model comparison of NO_x scaling factors

In the previous section, we created experiment-based averaged monthly scaling factors SF_{exp} for NO_2 and NO describing the daytime variation in stratospheric NO_x concentration above Zugspitze, Germany. Next, we compare the discussed results for SF_{exp} to model-based scaling factors SF_{sim} for NO_2 published by Strode et al. (2022) and for NO calculated from the same GEOS-GMI model simulation as the NO_2 scaling factors. Details of the GEOS model simulation with

GMI chemistry (Duncan et al., 2007; Strahan et al., 2007; Nielsen et al., 2017) are described in Strode et al. (2022) and references therein. The model parameters and the analysis method can be found in the literature (Strode et al., 2022). The given scaling factors $SF_{\text{sim}}(\text{NO}_2)$ and $SF_{\text{sim}}(\text{NO})$ are available for 146 levels between 6 and 78.5 km altitude in a 0.5 km grid and are normalized to $\text{SAZ} = 90^\circ$ (sunrise). For a better comparison of the experiment and model, we calculated mean values for SF_{sim} which also represent the stratospheric partial column above 16 km altitude. In order to do so, for each model level z , $SF_{\text{sim}}(z)$ was weighted to the mean monthly partial column profile of the given NO_x retrieval at z , and $SF_{\text{sim}}(> 16 \text{ km})$ was obtained via averaging over $SF_{\text{sim}}(16 \text{ km})$ to $SF_{\text{sim}}(78.5 \text{ km})$. Furthermore, $SF_{\text{sim}}(> 16 \text{ km})$ was normalized to $\text{SAZ} = 72^\circ$ (rather than sunrise/sunset), as done for SF_{exp} in Sect. 4.

$SF_{\text{sim}}(\text{NO}_2)$ and $SF_{\text{sim}}(\text{NO})$ are additionally shown in Figs. 5 and 6, respectively (red line). At first glance, SF_{exp} (black symbols) and SF_{sim} (red line) fit together very well, and the model data follow the experimental daytime variation for both NO_2 and NO.

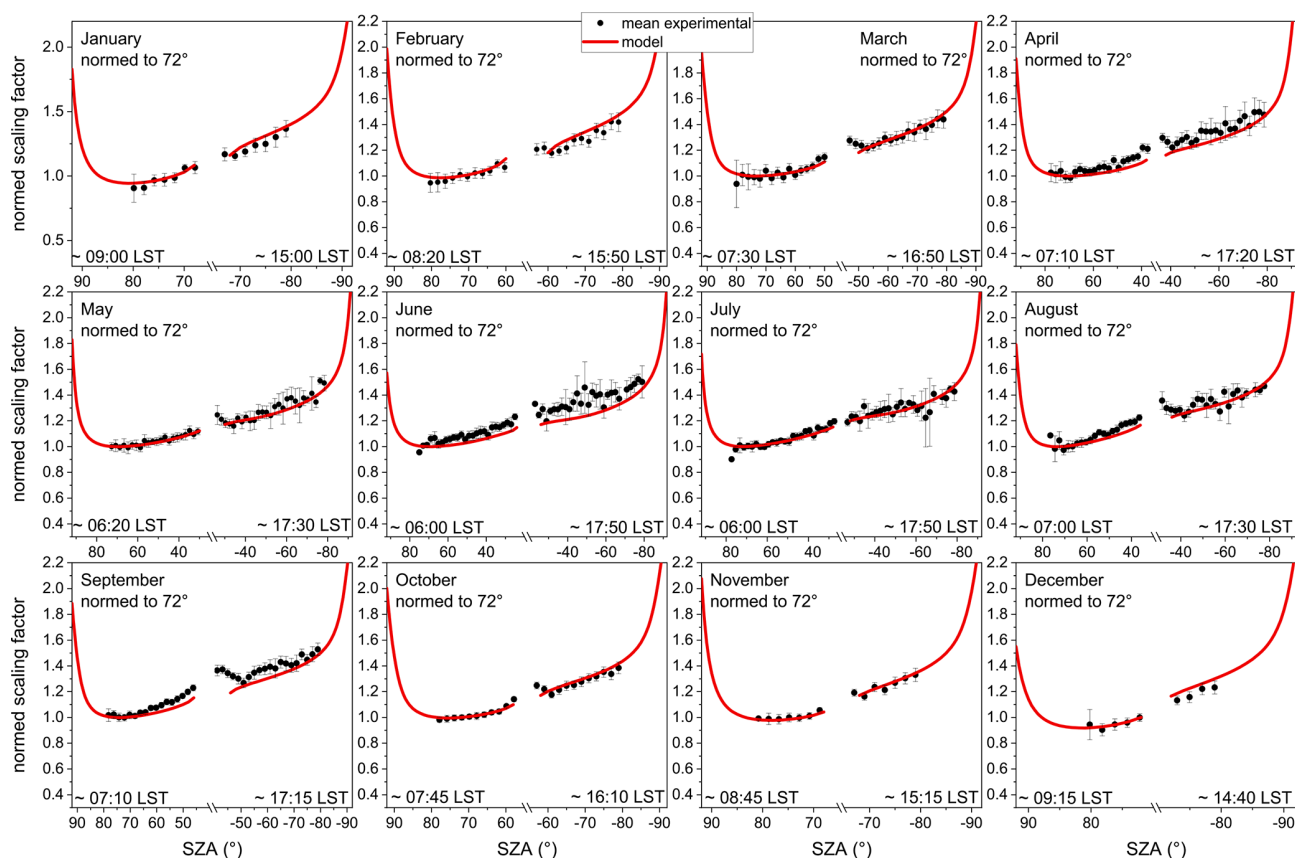


Figure 5. Calculated normalized NO₂ scaling factors $SF_{\text{exp}}(\text{NO}_2)$ above 16 km altitude measured at Zugspitze (black) and recalculated normalized NO₂ scaling factors $SF_{\text{sim}}(\text{NO}_2)$ above 16 km altitude (red line) for every month with respect to SZA. The experimental values represent the mean value within 2° SZA bins. The error bars represent 2 times the standard error of the mean ($\pm 2\sigma/\sqrt{n}$) value.

Quantitative evaluation

For the quantitative evaluation of the model comparison, the residuals between the experiment and model ($SF_{\text{exp}} - SF_{\text{sim}}/SF_{\text{sim}}$) are calculated for $SF(\text{NO}_2)$ and $SF(\text{NO})$ and are shown in Figs. 7 and 8, respectively. Additionally, the mean bias per month is shown as a mean value over all SZAs (dotted red line).

The residuals of $SF(\text{NO}_2)$ (Fig. 7) show over the whole year very good agreement between the experiment and model within $\pm 0.2\%$, reflecting the high quality of the GEOS-GMI simulation at midlatitudes. Significant differences between the experiment and model are visible only for a few months. For April, August and September, the morning increase in NO₂ is less pronounced in the model, leading to a significant deviation from the experimental values and an underestimation of the experiment-based scaling factors SF_{exp} at noon. However, the experimental values describing the stratospheric NO₂ variability can also be influenced by tropospheric variations because the NO₂ partial column used cannot be treated as completely independent of the tropospheric partial column (see Nürnberg et al., 2024). Furthermore, the model data have higher uncertainties during twi-

light, which can lead to deviations from the experiment (Alvanos and Christoudias, 2019).

Table 1 shows the mean bias (see also Fig. 7, dotted red line) for every month calculated from the residuals shown in Fig. 7 together with 2 times the SEM ($2\sigma/\sqrt{n}$). Unfortunately, due to the small values of 2 SEM of 0.0065% to 0.0192% for most of the months (except March, July, October, November), 2 SEM is smaller than the mean bias. Therefore, when taking 2 SEM as a quantitative indicator, SF_{exp} and SF_{sim} agree only in 4 months within the margin of error. However, when considering the mean deviation between the experiment and model of below $|0.068\%|$ per month, we can state that the model data published by Strode et al. (2022) reflect the experimental values retrieved from solar FTIR measurements at midlatitudes sufficiently well.

A very similar behavior can be obtained for $SF(\text{NO})$ (Fig. 8). With a maximum deviation of $\pm 0.2\%$, the agreement between the experiment and model is very similar, as seen for NO₂. However, it is remarkable that for the months with the highest SZA (January, February), the first data points after sunrise for which measurements exist (high-SZA region) deviate significantly from 0. Compared to Fig. 6, the

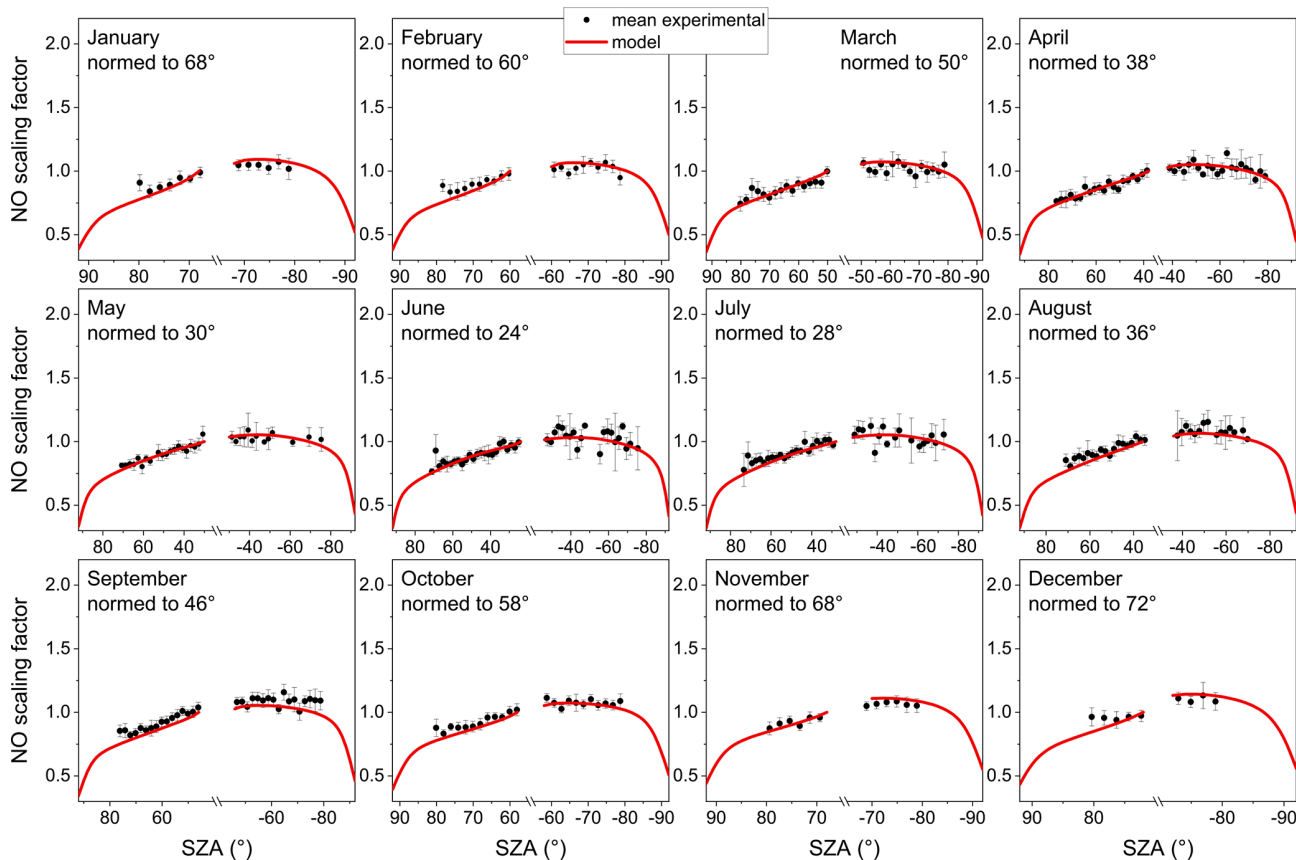


Figure 6. Calculated normalized NO scaling factors $SF_{\text{exp}}(\text{NO})$ above 16 km altitude measured at Zugspitze (black) and recalculated normalized NO scaling factors $SF_{\text{sim}}(\text{NO})$ above 16 km altitude (red line) for every month with respect to SZA. The experimental values represent the mean value within 2° SZA bins. The error bars represent 2 times the standard error of the mean ($\pm 2\sigma/\sqrt{n}$) value.

Table 1. Calculated mean bias of residuals ($[SF_{\text{exp}} - SF_{\text{sim}}]/SF_{\text{sim}}$) for every month between the experiment and simulations for NO₂ and 2 times the standard error of the mean ($2\sigma/\sqrt{n}$) of this value.

Month	J (%)	F (%)	M (%)	A (%)	M (%)	J (%)	J (%)	A (%)	S (%)	O (%)	N (%)	D (%)
Mean bias	-0.0230	-0.0257	-0.0024	0.0433	0.0118	0.0683	0.0060	0.0207	0.0414	-0.0062	0.0007	-0.0204
$2\sigma/\sqrt{n}$	0.0132	0.0092	0.0088	0.0082	0.0065	0.0096	0.0077	0.0093	0.0081	0.0072	0.0085	0.0192
Bias < 2 SEM?	No	No	Yes	No	No	No	Yes	No	No	Yes	Yes	No

experimental values in this region do not seem to follow the continuous increase expected from model descriptions. Here, an error source of the experimental data can be the wide range in photochemical regimes along the line of sight of the FTIR slant column measurements at high SZA: high up in the atmosphere, the sun is already well above the horizon, so there has already been significant NO production, while lower down the atmosphere is still much darker, and NO levels are still lower. The FTIR retrieval leads to an averaging over these effects because NO slant columns along the line of sight are retrieved from the solar measurements, and these are then converted to vertical column densities using a simple $\cos(\text{SZA})$ air mass correction.

Furthermore, the NO increase in the morning is more pronounced in the model, leading to a significant deviation from the experimental values and an overestimation of the experiment-based scaling factors SF_{exp} at noon. In the same manner as discussed before for NO₂, the experimental values describing the stratospheric NO variability can be influenced by tropospheric variations because the NO partial column used cannot be treated as completely independent of the tropospheric partial column (see Nürnberg et al., 2024). Consequently, the lower-stratospheric partial column in the morning is more influenced by the tropospheric partial column than in the evening.

In the same way as done for NO₂, the mean bias (see also Fig. 8, dotted red line) and $2\sigma/\sqrt{n}$ (2 SEM) are calcu-

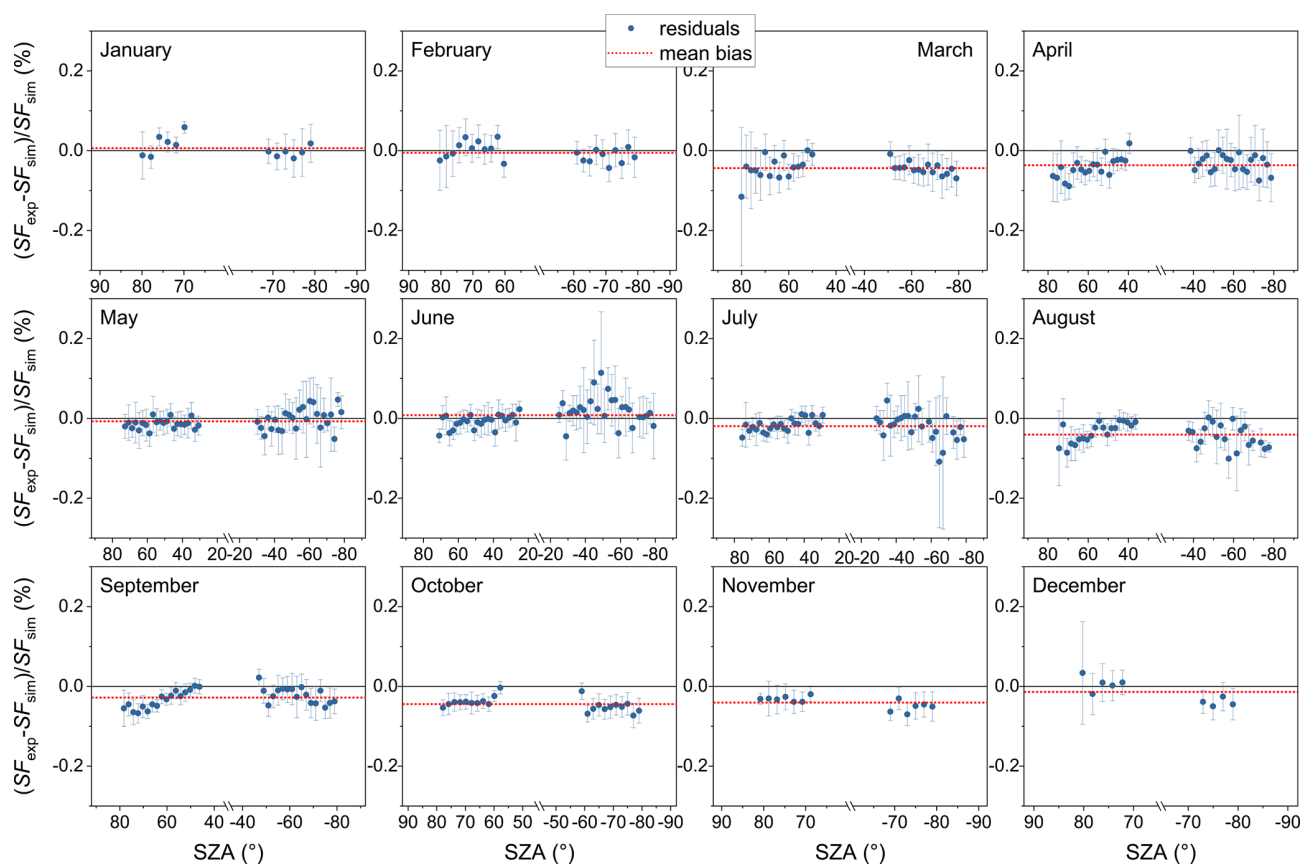


Figure 7. Calculated residuals $(SF_{\text{exp}} - SF_{\text{sim}})/SF_{\text{sim}}$ between the experimental normalized mean NO₂ scaling factors SF_{exp} and the simulated normalized NO₂ scaling factors SF_{sim} , interpolated to the respective SAZ for every month with respect to SAZ. The error bars represent 2 times the propagated standard error of the mean ($\pm 2\sigma/\sqrt{n}$) of the experimental value. The mean bias over all SAZs is shown in red.

Table 2. Calculated mean bias of residuals $([SF_{\text{exp}} - SF_{\text{sim}}]/SF_{\text{sim}})$ for every month between the experiment and simulations for NO and 2 times the standard error of the mean ($2\sigma/\sqrt{n}$) of this value.

Month	J (%)	F (%)	M (%)	A (%)	M (%)	J (%)	J (%)	A (%)	S (%)	O (%)	N (%)	D (%)
Mean bias	−0.0045	−0.0592	−0.0220	−0.0269	−0.0714	−0.0046	−0.0889	−0.0767	−0.0068	−0.0118	−0.0096	0.0150
$2\sigma/\sqrt{n}$	0.0331	0.0236	0.0166	0.0110	0.0099	0.0160	0.0143	0.0102	0.0117	0.0138	0.0191	0.0425
Bias < 2 SEM?	Yes	No	No	No	No	Yes	No	No	Yes	Yes	Yes	Yes

lated and are shown in Table 2 for the NO residuals. Here, better agreement between the experiment and model can be quantified. For 6 months (January, June, September, October, November, December) the mean bias is smaller than 2 SEM, indicating agreement between the experiment and model within the error bars. Nevertheless, this observation not only reflects better agreement between the experiment and model but can also be explained by a higher scattering of the residuals, leading to a higher SEM. This can be confirmed when comparing the values for 2 SEM given in Tables 1 and 2. With a mean 2 SEM of the residuals over all months of 0.0096 % for NO₂ and 0.0185 % for NO, the residual scattering with a similar n and a similar mean bias of 0.02 % is 2 times larger for NO.

In conclusion, the quantitative comparison of the experimental-derived scaling factors SF_{exp} and the scaling factors derived from model simulations SF_{sim} for NO₂ and NO showed very good agreement between both data sets, with a mean bias between the experiment and model of only 0.02 % over all months, underlining the quality of the model data at midlatitudes and the reliability of the retrieved experiment-based scaling factors.

6 Summary and conclusions

In this work, we reanalyzed an experimental long-term data set from solar FTIR measurements over 25 years of measurement at Zugspitze (47.42° N, 10.98° E; 2964 m a.s.l.), Ger-

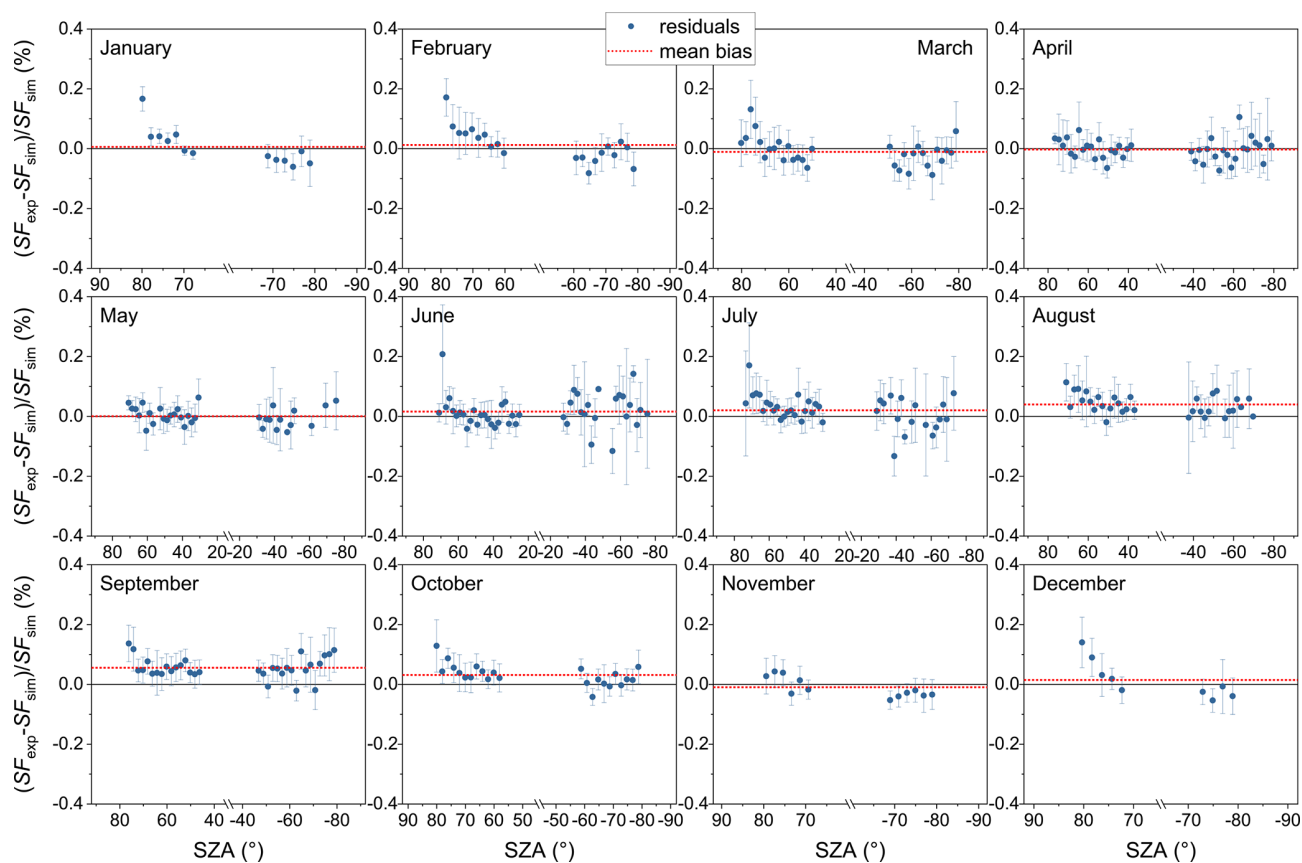


Figure 8. Calculated residuals ($(SF_{\text{exp}} - SF_{\text{sim}}) / SF_{\text{sim}}$) between the experimental normalized mean NO scaling factors SF_{exp} and the simulated normalized NO scaling factors SF_{sim} , interpolated to the respective SZA for every month with respect to SZA. The error bars represent 2 times the propagated standard error of the mean ($\pm 2\sigma / \sqrt{n}$) of the experimental value. The mean bias over all SZAs is shown in red.

many, published in a companion paper (Part 1, Nürnberg et al., 2024). We present for the first time experiment-based scaling factors SF_{exp} as a function of the solar zenith angle (SZA), representing monthly daytime NO₂ and NO variabilities in the stratosphere (> 16 km altitude) within time steps of minutes. SF_{exp} is a measure of the variability of the NO_x partial column above 16 km altitude in comparison to local solar noon. We calculated SF_{exp} from the time-dependent monthly NO_x partial columns (published in Part 1) by averaging over SZA bins of 2° and a normalization to SZA = 72°. The resulting values of $SF_{\text{exp}}(\text{NO}_2)$ and $SF_{\text{exp}}(\text{NO})$ reflect the expected daytime variability of NO₂ and NO described in Part 1 very well (Nürnberg et al., 2024). Only the boundary values in spring and autumn months deviate significantly due to the relatively fast change in the minimum SZA during these months, which influences the average value. Neglecting these values leads to two reliable experiment-based data sets for $SF_{\text{exp}}(\text{NO}_2)$ and $SF_{\text{exp}}(\text{NO})$. Furthermore, we used these new experiment-based data sets to validate recently published simulation-based scaling factors $SF_{\text{sim}}(\text{NO}_2)$ (Strode et al., 2022) and recently calculated simulation-based scaling factors $SF_{\text{sim}}(\text{NO})$ from a global study representing a similar

latitude (47° N). Comparing the experiment and model simulation, we find excellent agreement for stratospheric NO₂ and NO daytime variabilities, with a mean bias of the modulus over all months and SZA of only 0.02 %, with no significant deviating trends for boundary values. These results underline the quality of recent multi-dimensional model simulations of stratospheric trace gases, representing experimental data very well. Additionally, we showed that ground-based FTIR measurements can provide reliable information about stratospheric NO_x variability within time steps of minutes, which can serve as a good basis for the validation of global model simulations and can therefore help to further optimize satellite validations.

The analysis method for retrieving stratospheric NO₂ and NO partial columns over Zugspitze, Germany, published in Part 1 (Nürnberg et al., 2024), combined with the generalization of this data by calculating unitless scaling factors (SFs) and the validation of recently published model data in this paper (Part 2), can be seen as a useful tool for the further validation and correction of global model and satellite data. This approach can be taken for any ground-based FTIR spectrometer generating a global set of experiment-based stratospheric

NO₂ and NO partial columns or scaling factors SF_{exp}(NO₂) and SF_{exp}(NO).

Data availability. The presented calculated experimental factors SF_{exp} and the partial columns used as a function of the SZA can be found in the Supplement of this paper. The experimental data used are published in Part 1 (Nürnberg et al., 2024). Any other data of interest underlying this publication can be obtained at any time from the corresponding author upon request. The simulated scaling factors for NO₂ and NO are available at https://avdc.gsfc.nasa.gov/pub/data/project/GMI_SF/ (Strode, 2021).

Supplement. The supplement related to this article is available online at: <https://doi.org/10.5194/acp-24-10001-2024-supplement>.

Author contributions. PN optimized and performed the FTIR retrievals, conducted the scientific analysis, and wrote the paper. SAS performed the model simulations, processed the data for comparison to the experiment and assisted in editing the paper. RS proposed this research, contributed to the design of the study and assisted in editing the paper.

Competing interests. The contact author has declared that none of the authors has any competing interests.

Disclaimer. Publisher's note: Copernicus Publications remains neutral with regard to jurisdictional claims made in the text, published maps, institutional affiliations, or any other geographical representation in this paper. While Copernicus Publications makes every effort to include appropriate place names, the final responsibility lies with the authors.

Acknowledgements. Sarah A. Strode acknowledges the possibility of using computing resources from the NASA Center for Climate Simulation (NCCS) for the simulated scaling factors.

Financial support. This work was funded by the Federal Ministry of Education and Research of Germany within the ACTRIS-D project (grant no. 01LK2001B) and by the Helmholtz Changing Earth – Sustaining our Future research program within the Earth and Environment research field. Sarah A. Strode was supported by NASA (grant no. 80NSSC18K0711) as a part of the NASA Modeling, Analysis, and Prediction (MAP) program.

The article processing charges for this open-access publication were covered by the Karlsruhe Institute of Technology (KIT).

Review statement. This paper was edited by Rolf Müller and reviewed by Tijnl Verhoelst and one anonymous referee.

References

- Allen, M., Lunine, J. I., and Yung, Y. L.: The vertical distribution of ozone in the mesosphere and lower thermosphere, *J. Geophys. Res.*, 89, 4841–4872, <https://doi.org/10.1029/JD089iD03p04841>, 1984.
- Alvanos, M. and Christoudias, T.: Accelerating Atmospheric Chemical Kinetics for Climate Simulations, *IEEE T. Parallel. Distrib. Syst.*, 30, 2396–2407, <https://doi.org/10.1109/TPDS.2019.2918798>, 2019.
- Bracher, A., Sinnhuber, M., Rozanov, A., and Burrows, J. P.: Using a photochemical model for the validation of NO₂ satellite measurements at different solar zenith angles, *Atmos. Chem. Phys.*, 5, 393–408, <https://doi.org/10.5194/acp-5-393-2005>, 2005.
- Brohede, S. M., Haley, C. S., McLinden, C. A., Sioris, C. E., Murtagh, D. P., Petelina, S. V., Llewellyn, E. J., Bazureau, A., Goutail, F., Randall, C. E., Lumpe, J. D., Taha, G., Thomasson, L. W., and Gordley, L. L.: Validation of Odin/OSIRIS stratospheric NO₂ profiles, *J. Geophys. Res.-Atmos.*, 112, D07310, <https://doi.org/10.1029/2006JD007586>, 2007.
- Chang, J. and Duewer, W. H.: Modeling chemical processes in the stratosphere, *Annu. Rev. Phys. Chem.*, 30, 443–469, 1979.
- Crutzen, P. J.: The influence of nitrogen oxides on the atmospheric ozone content, *Q. J. Roy. Meteor. Soc.*, 96, 320–325, <https://doi.org/10.1002/qj.49709640815>, 1970.
- Crutzen, P. J.: The Role of NO and NO₂ in the Chemistry of the Troposphere and Stratosphere, *Annu. Rev. Earth Planet. Sc.*, 7, 443–472, <https://doi.org/10.1146/annurev.ea.07.050179.002303>, 1979.
- Dubé, K., Randel, W., Bourassa, A., Zawada, D., McLinden, C., and Degenstein, D.: Trends and Variability in Stratospheric NO_x Derived From Merged SAGE II and OSIRIS Satellite Observations, *J. Geophys. Res.-Atmos.*, 125, e2019JD031798, <https://doi.org/10.1029/2019jd031798>, 2020.
- Dubé, K., Bourassa, A., Zawada, D., Degenstein, D., Damadeo, R., Flittner, D., and Randel, W.: Accounting for the photochemical variation in stratospheric NO₂ in the SAGE III/ISS solar occultation retrieval, *Atmos. Meas. Tech.*, 14, 557–566, <https://doi.org/10.5194/amt-14-557-2021>, 2021.
- Duncan, B. N., Strahan, S. E., Yoshida, Y., Steenrod, S. D., and Livesey, N.: Model study of the cross-tropopause transport of biomass burning pollution, *Atmos. Chem. Phys.*, 7, 3713–3736, <https://doi.org/10.5194/acp-7-3713-2007>, 2007.
- Godin-Beekmann, S.: Spatial observation of the ozone layer, *C. R. Geosci.*, 342, 339–348, <https://doi.org/10.1016/j.crte.2009.10.012>, 2010.
- Grewe, V., Brunner, D., Dameris, M., Grenfell, J. L., Hein, R., Shindell, D., and Staehelin, J.: Origin and variability of upper tropospheric nitrogen oxides and ozone at northern mid-latitudes, *Atmos. Environ.*, 35, 3421–3433, [https://doi.org/10.1016/s1352-2310\(01\)00134-0](https://doi.org/10.1016/s1352-2310(01)00134-0), 2001.
- Johnston, H. S.: Atmospheric ozone, *Annu. Rev. Phys. Chem.*, 43, 1–31, <https://doi.org/10.1146/annurev.pc.43.100192.000245>, 1992.
- McLinden, C. A., Olsen, S. C., Hannegan, B., Wild, O., Prather, M. J., and Sundet, J.: Stratospheric ozone in 3-D models: A simple chemistry and the cross-tropopause flux, *J. Geophys. Res.-Atmos.*, 105, 14653–14665, <https://doi.org/10.1029/2000jd900124>, 2000.

- Nielsen, J. E., Pawson, S., Molod, A., Auer, B., da Silva, A. M., Douglass, A. R., Duncan, B., Liang, Q., Manyin, M., Oman, L. D., Putman, W., Strahan, S. E., and Wargan, K.: Chemical Mechanisms and Their Applications in the Goddard Earth Observing System (GEOS) Earth System Model, *J. Adv. Model. Earth Sy.*, 9, 3019–3044, <https://doi.org/10.1002/2017MS001011>, 2017.
- Nürnberg, P., Rettinger, M., and Sussmann, R.: Solar FTIR measurements of NO_x vertical distributions – Part 1: First observational evidence of a seasonal variation in the diurnal increasing rates of stratospheric NO₂ and NO, *Atmos. Chem. Phys.*, 24, 3743–3757, <https://doi.org/10.5194/acp-24-3743-2024>, 2024.
- Prather, M. and Jaffe, A. H.: Global impact of the Antarctic ozone hole: Chemical propagation, *J. Geophys. Res.*, 95, 3473–3492, <https://doi.org/10.1029/JD095iD04p03473>, 1990.
- Richter, A. and Burrows, J. P.: Tropospheric NO₂ from GOME measurements, *Adv. Space Res.*, 29, 1673–1683, [https://doi.org/10.1016/s0273-1177\(02\)00100-x](https://doi.org/10.1016/s0273-1177(02)00100-x), 2002.
- Rinsland, C. P., Boughner, R. E., Larsen, J. C., Stokes, G. M., and Brault, J. W.: Diurnal variations of atmospheric nitric oxide: Ground-based infrared spectroscopic measurements and their interpretation with time-dependent photochemical model calculations, *J. Geophys. Res.*, 89, 9613–9622, <https://doi.org/10.1029/JD089iD06p09613>, 1984.
- Rusch, D. W.: Satellite ultraviolet measurements of nitric oxide fluorescence with a diffusive transport model, *J. Geophys. Res.*, 78, 5676–5686, <https://doi.org/10.1029/JA078i025p05676>, 1973.
- Solomon, S., Portmann, R. W., Sanders, R. W., Daniel, J. S., Madsen, W., Bartram, B., and Dutton, E. G.: On the role of nitrogen dioxide in the absorption of solar radiation, *J. Geophys. Res.-Atmos.*, 104, 12047–12058, <https://doi.org/10.1029/1999jd900035>, 1999.
- Strahan, S. E., Duncan, B. N., and Hoor, P.: Observationally derived transport diagnostics for the lowermost stratosphere and their application to the GMI chemistry and transport model, *Atmos. Chem. Phys.*, 7, 2435–2445, <https://doi.org/10.5194/acp-7-2435-2007>, 2007.
- Strode, S.: Diurnal Scaling Factors, NASA [data set], https://avdc.gsfc.nasa.gov/pub/data/project/GMI_SF/ (last access: 12 July 2024), 2021.
- Strode, S. A., Taha, G., Oman, L. D., Damadeo, R., Flittner, D., Schoeberl, M., Sioris, C. E., and Stauffer, R.: SAGE III/ISS ozone and NO₂ validation using diurnal scaling factors, *Atmos. Meas. Tech.*, 15, 6145–6161, <https://doi.org/10.5194/amt-15-6145-2022>, 2022.
- Sussmann, R., Stremme, W., Burrows, J. P., Richter, A., Seiler, W., and Rettinger, M.: Stratospheric and tropospheric NO₂ variability on the diurnal and annual scale: a combined retrieval from ENVISAT/SCIAMACHY and solar FTIR at the Permanent Ground-Truthing Facility Zugspitze/Garmisch, *Atmos. Chem. Phys.*, 5, 2657–2677, <https://doi.org/10.5194/acp-5-2657-2005>, 2005.
- Wang, S., Li, K.-F., Zhu, D., Sander, S. P., Yung, Y. L., Pazmino, A., and Querel, R.: Solar 11-Year Cycle Signal in Stratospheric Nitrogen Dioxide—Similarities and Discrepancies Between Model and NDACC Observations, *Sol. Phys.*, 295, 117, <https://doi.org/10.1007/s11207-020-01685-1>, 2020.
- World Health Organization: Regional Office for Europe: Health aspects of air pollution with particulate matter, ozone and nitrogen dioxide: report on a WHO working group, Bonn, Germany, 13–15 January 2003, Copenhagen: WHO Regional Office for Europe, <https://apps.who.int/iris/handle/10665/107478> (last access: 19 July 2024), 2003.
- Yin, H., Sun, Y., Liu, C., Zhang, L., Lu, X., Wang, W., Shan, C., Hu, Q., Tian, Y., Zhang, C., Su, W., Zhang, H., Palm, M., Notholt, J., and Liu, J.: FTIR time series of stratospheric NO₂ over Hefei, China, and comparisons with OMI and GEOS-Chem model data, *Opt. Express*, 27, A1225–A1240, <https://doi.org/10.1364/OE.27.0A1225>, 2019.
- Zhou, M., Langerock, B., Vigouroux, C., Dils, B., Hermans, C., Kumps, N., Nan, W., Metzger, J.-M., Mahieu, E., Wang, T., Wang, P., and De Mazière, M.: Tropospheric and stratospheric NO retrieved from ground-based Fourier-transform infrared (FTIR) measurements, *Atmos. Meas. Tech.*, 14, 6233–6247, <https://doi.org/10.5194/amt-14-6233-2021>, 2021.